PRAMANA
— journal of
physics

Vol. 77, No. 6
December 2011
pp. 1095–1104

On the elliptic flow for nearly symmetric collisions and nuclear equation of state

VARINDERJIT KAUR and SUNEEL KUMAR*
School of Physics and Material Science, Thapar University, Patiala 147 004, India
*Corresponding author. E-mail: suneel.kumar@thapar.edu

MS received 22 November 2010; revised 31 March 2011; accepted 4 May 2011

Abstract. We present the results of elliptic flow for the collision of nearly symmetric nuclei ($_{10}Ne^{20} + _{13}Al^{27}$, $_{18}Ar^{40} + _{21}Sc^{45}$, $_{30}Zn^{64} + _{28}Ni^{58}$, $_{36}Kr^{86} + _{41}Nb^{93}$) using the quantum molecular dynamics (QMD) model. General features of elliptic flow are investigated with the help of theoretical simulations. The simulations are performed at beam energies between 45 and 105 MeV/nucleon. A significant change can be seen from in-plane to out-of-plane elliptic flow of different fragments with incident energy. A comparison with experimental data is also made. Further, we show that elliptic flow for different fragments follows power-law dependence as given by the function $C(A_{\rm tot})^{\tau}$.

Keywords. Elliptic flow; nearly symmetric nuclei; quantum molecular dynamics; light mass fragments.

PACS Nos 25.70.Pq; 25.70.−z; 24.10.Lx

1. Introduction

Heavy-ion collisions at intermediate energies have captured the centre place in the present day nuclear research because of the several rare phenomena emerging at these incident energies and their utility in several other branches of physics [1–4]. The nuclear equation of state (EOS) is hoped to be pindown via the liquid–gas transition, multi-fragmentation and anisotropic flows, such as directed and elliptic flows produced in heavy-ion collisions [5,6]. Such knowledge is not only of interest in nuclear physics but is also useful in understanding astrophysical phenomena such as supernova explosions and neutron stars. One observable that has been used extensively for extracting the nuclear EOS from heavy-ion collisions is the anisotropic flow of various particles.

In recent years, the anisotropic flow at intermediate energies has attracted increasing attention of the heavy-ion community because the anisotropic flow [6,7] is very sensitive to the early evolution of the system [7–9]. The anisotropic flow is defined as the azimuthal asymmetry in the particle distribution with respect to the reaction plane (the plane spanned by the beam direction and impact parameter vector). This gives the magnitude of the

DOI: 10.1007/s12043-011-0147-7; ***e*Publication: 4 October 2011**

asymmetry and is characterized by the Fourier expansion of the azimuthal distribution [10] of the detected particles at midrapidities as

$$\frac{\mathrm{d}N}{\mathrm{d}\phi} = p_0(1 + 2V_1 \cos\phi + 2V_2 \cos 2\phi).$$

Here ϕ is the azimuthal angle between the transverse momentum of the particle and reaction plane. The first harmonic term describes the so-called directed flow which is the bounce-off of cold spectator matter in the reaction plane [11] and the second harmonic term corresponds to the elliptic flow which is the squeeze-out of the hot and compressed participant matter perpendicular to the reaction plane [12–14]. The corresponding Fourier coefficients, V_n, are used to quantify this effect [10]. These two observables together represent the anisotropic part of the transverse flow and appear only in the non-central heavy-ion collisions. The elliptic flow [10] has been proven to be one of the most fruitful probes for extracting the equation of state (EOS) and to study the dynamics of heavy-ion collisions that originate from the almond-shaped region of the overlap zone and is produced by the unequal pressure gradients, i.e. an anisotropy in the transverse momentum direction. V_2 can also be expressed as

$$V_2 = \left\langle \frac{P_x^2 - P_y^2}{P_x^2 + P_y^2} \right\rangle,$$

where P_x and P_y are the components of the momentum along the x-and y-axes, respectively.

The positive value of V_2 describes the eccentricity of an ellipse like distribution and indicates the in-plane enhancement of the particle emission, i.e. a rotational behaviour. Note that isotropy of the space requires that V_2 should vanish. Obviously, zero value of V_2 corresponds to an isotropic distribution in the transverse plane. Since elliptic flow develops at a very early stage of the nuclear collision, it is an excellent tool to probe the nuclear equation of state (EOS) under the extreme conditions of temperature and density.

Many theoretical and experimental efforts have been made in studying the collective transverse flow in heavy-ion collisions at intermediate energies [8,15–17]. In 1982, Stöcker *et al* were the first to predict the midrapidity emission perpendicular to the reaction plane [12]. At the same time, Gyulassy *et al* [18] put forward the kinetic energy tensor to analyse the flow patterns. Experimentally observed out-of-plane emission, termed as squeeze-out, was first observed by Diogene Collaboration [19]. The Plastic Ball group at the Bevalac in Berkley were the first to quantify the squeeze-in symmetric systems. They studied Au + Au collisions at 400 MeV/nucleon [20]. Furthermore, the transition from the in-plane to out-of-plane emission was first observed by the NAUTILUS Collaboration at GANIL in 1994 using Zn + Ni reaction [21]. Theoretically, many important develpments in this area, e.g. the dependencies of elliptic flow on the impact parameter and transverse momentum have been determined. These main features have been confirmed by the FOPI, INDRA and ALADIN Collaborations [22,23]. The MINIBALL/ALADIN Collaboration also observed the onset of out-of-plane emission in Au + Au collisions at 100 MeV/nucleon [13]. In most of these studies, $_{79}\mathrm{Au}^{197}$ + $_{79}\mathrm{Au}^{197}$ reactions have been chosen [22,23]. The elliptic flow at incident energies from tens to hundreds of MeV/nucleon are determined by the complex interplay among expansion, rotation and the shadowing of spectators [24]. Both the mean-field and two-body collision parts (real and imaginary parts of G-matrix) play

equally important roles in this energy domain. The mean field plays a dominant role at low incident energies, and then gradually the two-body collision becomes dominant as the incident energy increases. A detailed study of the excitation function of elliptic flow, in this energy region, therefore, can provide useful information on the nature of nucleon–nucleon interaction related to the equation of state. Interestingly, a systematic theoretical study of the elliptic flow for nearly symmetric systems is still very rare [25]. In this paper, we attempt to study the different aspects of elliptic flow V_2 for nearly symmetric systems ($A_P \neq A_T$), e.g., ${}_{10}\mathrm{Ne}^{20} + {}_{13}\mathrm{Al}^{27}$, ${}_{18}\mathrm{Ar}^{40} + {}_{21}\mathrm{Sc}^{45}$, ${}_{30}\mathrm{Zn}^{64} + {}_{28}\mathrm{Ni}^{58}$, ${}_{36}\mathrm{Kr}^{86} + {}_{41}\mathrm{Nb}^{93}$ within the framework of quantum molecular dynamics (QMD) model which is explained in ref. [3]. This model is used to generate the phase space of nucleons. The article is organized as follows: A brief description of the model is given in §2. Our results are discussed in §3. Finally, we summarize the results in §4.

2. Quantum molecular dynamics (QMD) model

The quantum molecular dynamics (QMD) model is a time-dependent many-body theoretical approach which is based on the molecular dynamics picture that treats nuclear correlations explicitly. The two dynamical ingredients of the model are the density-dependent mean field and the in-medium nucleon–nucleon cross-section [26]. In the QMD model, each nucleon is represented by a Gaussian wave packet characterized by the time-dependent parameters in space $\vec{r}_i(t)$ and in momentum $\vec{p}_i(t)$ [3]. This wave packet is represented as

$$\Phi_i(\vec{r}, \vec{p}, t) = \frac{1}{(2\pi L)^{3/4}} \mathrm{e}^{\frac{-(\vec{r}-\vec{r}_i(t))^2}{2L}} \mathrm{e}^{\frac{i\vec{p}_i(t).\vec{r}}{\hbar}}. \tag{1}$$

The centroid of each nucleon propagates under the classical Hamilton equations of motion [3].

$$\frac{\mathrm{d}\vec{r}_i}{\mathrm{d}t} = \frac{\mathrm{d}H}{\mathrm{d}\vec{p}_i}; \quad \frac{\mathrm{d}\vec{p}_i}{\mathrm{d}t} = -\frac{\mathrm{d}H}{\mathrm{d}\vec{r}_i}. \tag{2}$$

Here H stands for the Hamiltonian which is given by

$$H = \sum_i \frac{p_i^2}{2m_i} + \sum_i (V^{\mathrm{Loc}} + V^{\mathrm{Yukawa}} + V^{\mathrm{Coul}}). \tag{3}$$

Here V^{Loc}, V^{Yukawa}, V^{Coul} represent, respectively, the Skyrme, Yukawa and Coulomb parts of the interaction. To understand the role of different compressibilities, a parametrized form of potential can be written as

$$U^{\mathrm{loc}} = \alpha \left(\frac{\rho}{\rho_0}\right) + \beta \left(\frac{\rho}{\rho_0}\right)^{\gamma}. \tag{4}$$

The parameters α, β and γ are listed in ref. [3].

3. Results and discussion

The main advantage of the QMD model is that it can explicitly represent the many-body states of the system and thus contains the correlation effects. Therefore, it provides important information about the collision dynamics.

In this paper, free nucleons and different fragments, i.e., light mass fragments (LMFs) ($2 \leq A \leq 4$) and intermediate mass fragments (IMFs) ($5 \leq A \leq A_{\rm tot}/6$) were selected for elliptic flow analysis. Some studies have been carried out for elliptic flow involving heavier fragments [27]. We performed a complete systematic study using the nearly symmetric reactions ${}_{10}Ne^{20} + {}_{13}Al^{27}$, ${}_{18}Ar^{40} + {}_{21}Sc^{45}$, ${}_{30}Zn^{64} + {}_{28}Ni^{58}$, ${}_{36}Kr^{86} + {}_{41}Nb^{93}$ at incident energies between 45 and 105 MeV/nucleon. We have simulated these reactions over the full collision geometry starting from the central to peripheral one. The fragments were constructed within the minimum spanning tree (MST) method [3]. The MST method binds two nucleons in a fragment if their distance is less than 4 fm. The entire calculations were performed at final state that is 200 fm/c. We also note that several different models on clusterization are also reported in recent publications [28].

In figure 1, the final-state elliptic flow is displayed for the free particles (upper panel), light mass fragments (LMFs) ($2 \leq A \leq 4$) (middle panel) and intermediate mass fragments

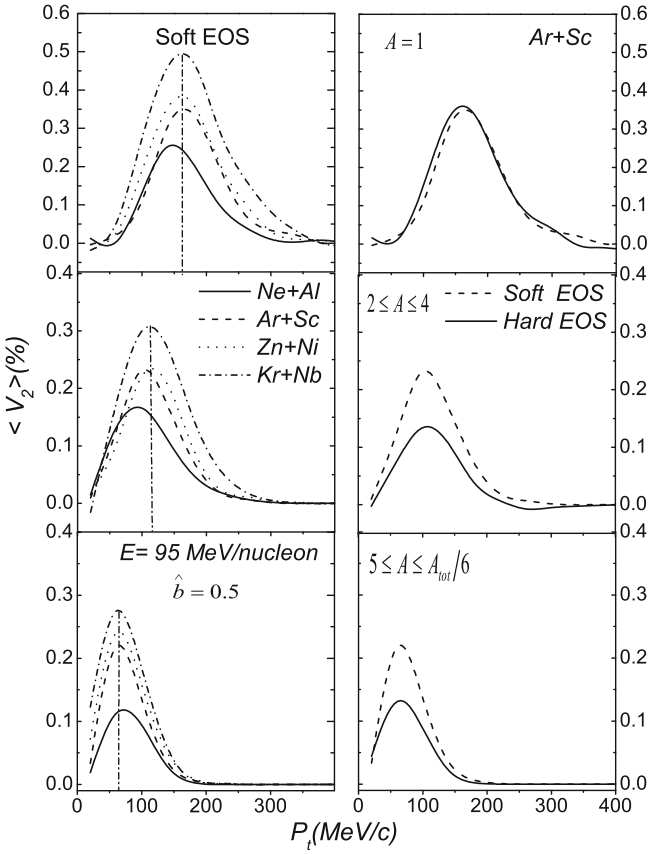

Figure 1. The elliptic flow as a function of the transverse momentum at incident energy 95 MeV/nucleon for free particles, LMFs and IMFs in top, middle and bottom panels respectively. On the right hand side, elliptic flow for soft and hard EOSs for Ar + Sc system is displayed.

(IMFs) ($5 \leq A \leq A_{\rm tot}/6$) (lower panel) at the scaled impact parameter $\hat{b} = 0.5$. One can see a Gaussian-type behaviour quite similar to the one reported by Colona and Toro *et al* [29]. This Gaussian-type behaviour is integrated over the entire rapidity range. There is a linear increase in the elliptic flow with transverse momentum upto certain P_t. Obviously particles with larger momentum will escape the reaction zone earlier. One also sees from the figure, that the elliptic flow of nucleons/LMFs/IMFs is positive in the whole range of P_t which signifies an in-plane emission. Moreover, collective rotation is one of the main mechanisms for inducing the positive elliptic flow in the whole range of P_t. It is also evident from the figure that the peaks of Gaussian shifts toward the lower value of P_t for heavier fragments because the emitted free and light mass fragments can feel the role of mean field directly, while the heavier fragments have weak sensitivity [30]. It is also evident from the figure that the reactions under consideration have different system mass dependence as well as N/Z ratios.

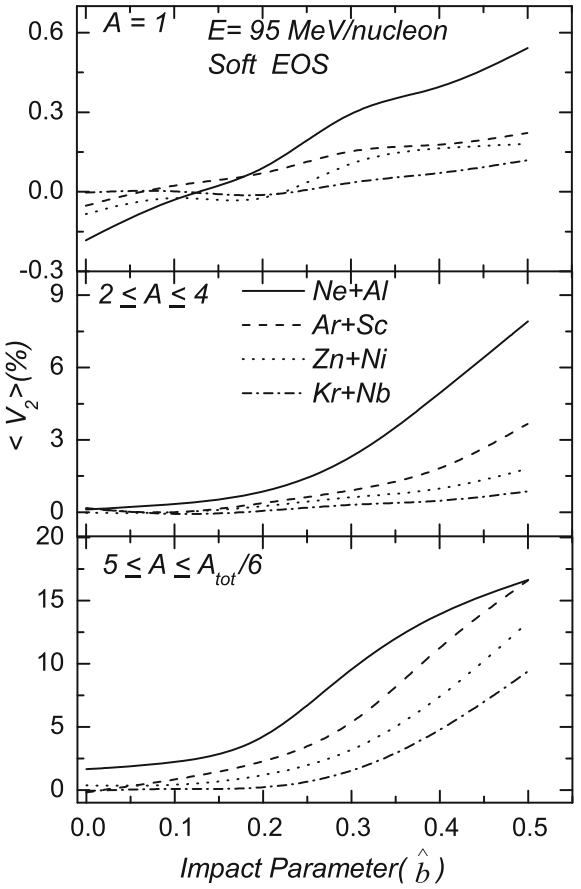

Figure 2. The elliptic flow as a function of impact parameter and at an incident energy $E = 95$ MeV/nucleon for free particles, LMFs and IMFs in top, middle and bottom panels respectively.

Moreover, the results are found to vary drastically with the change of equation of state. To make this point more clear, we have dislayed on the right-hand side of figure 1, the transverse momentum dependence of elliptic flow using soft and hard equations of state. For this analysis, we choose Ar + Sc reaction at $\hat{b} = 0.5$ and $E = 95$ MeV/nucleon. We can clearly see the effect of hard and soft equations of state in the production of light mass fragments (LMFs) and intermediate mass fragments (IMFs). On the contrary, very little change is observed in the case of free particles. This is due to the different compressibility values for hard EOS ($K = 380$ MeV) and soft EOS ($K = 200$ MeV).

The elliptic flows as a function of scaled impact parameter for the above-mentioned systems are displayed in figure 2. The simulations were carried out at 95 MeV/nucleon for the scaled impact parameter $\hat{b}$ between 0.0 and 0.5. The results for free nucleons (upper panel), LMFs (middle panel) and IMFs (lower panel) have been shown for all four systems considered in this analysis. The value of the elliptic flow V_2 becomes more positive (in-plane) with the impact parameter. There is an obvious difference among the elliptic flow

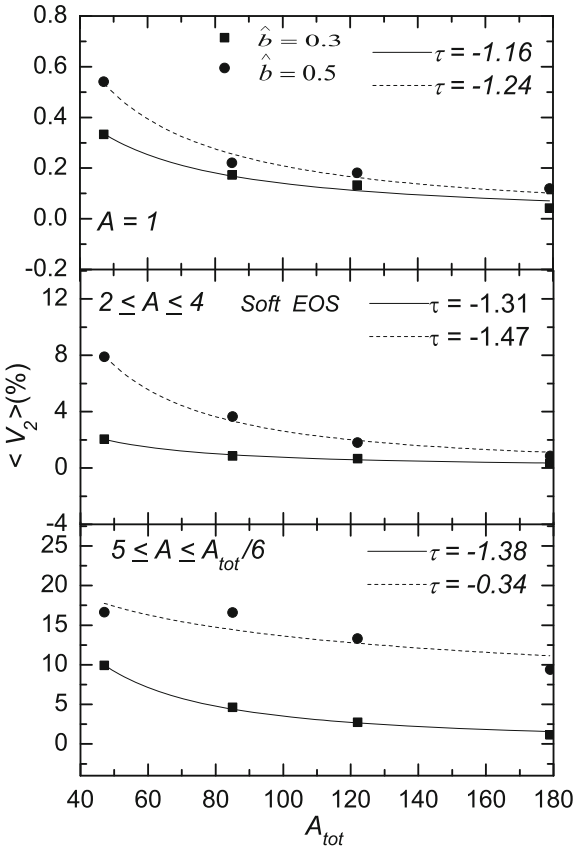

Figure 3. The dependence of elliptic flow on the composite mass of the systems for free nucleons, LMFs and IMFs in top, middle and bottom panels, respectively. The curves are fitted using an equation given by the function $C(A_{\rm tot})^{\tau}$.

associated with the free particles (upper panel), light mass fragments (LMFs) ($2 \leq A \leq 4$) (middle panel) and intermediate mass fragments (IMFs) ($5 \leq A \leq A_{\rm tot}/6$) (lower panel). This is more true at higher impact parameters. One can see the isotropic distribution of the fragments at small impact parameters which turns into anisotropic distribution as we move away towards semicentral zone. For lighter systems, the value of V_2 increases more rapidly with impact parameter. This is due to the azimuthal anisotropy, that becomes larger with the impact parameter and reduces with the beam energy. For semicentral collisions, less number of nucleons participate in the collision process which lead to more elliptic flow. Since the production of the intermediate mass fragments is due to the spectator part, the elliptic flow is stronger for the heavier fragments compared to the lighter fragments.

We further carry out the study of the system size dependence of the elliptic flow of free particles (upper panel), light mass fragments (LMFs) ($2 \leq A \leq 4$) (middle panel) and intermediate mass fragments (IMFs) ($5 \leq A \leq A_{\rm tot}/6$) (lower panel) for different reactions, namely ${}_{10}\mathrm{Ne}^{20} + {}_{13}\mathrm{Al}^{27}$, ${}_{18}\mathrm{Ar}^{40} + {}_{21}\mathrm{Sc}^{45}$, ${}_{30}\mathrm{Zn}^{64} + {}_{28}\mathrm{Ni}^{58}$, ${}_{36}\mathrm{Kr}^{86} + {}_{41}\mathrm{Nb}^{93}$ at two different impact parameters $\hat{b} = 0.3$ and 0.5 as shown in figure 3. The elliptic flow varies with the mass number. It has been shown that there is a linear relation between the system size and particle emission [20,27]. One can see that elliptic flow starts to approach negative value (i.e. squeeze-out) with composite mass of the system because the pressure produced by the Coulomb interactions increases with the system size, i.e. heavier systems have much larger Coulomb repulsion. This repulsion will force the fragments to go out-of-plane and hence the elliptic flow starts to approach negative value as one goes from lighter to heavier systems. On the other hand, elliptic flow is observed to be in-plane compared to out-of-plane at higher impact parameters. With the increase in the impact parameter, the

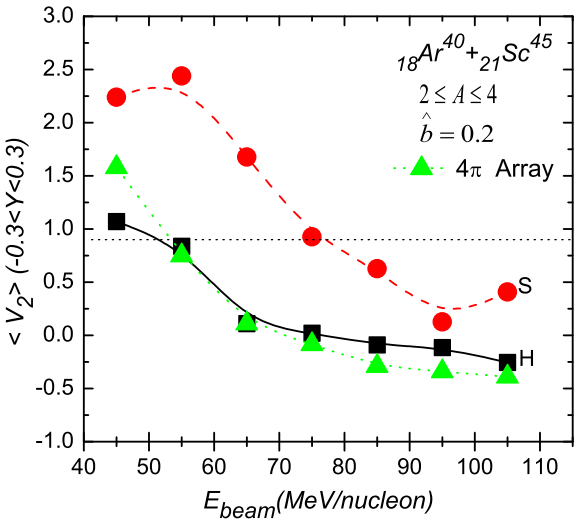

Figure 4. The variation of the elliptic flow with beam energy for the Ar + Sc reaction using hard and soft equations of state. Here comparison is shown with experimental findings of the 4π Array.

participant zone decreases, resulting in an increase in the spectator region, which will lead the fragments to enjoy in-plane as compared to out-of-plane. All the curves are fitted as given by the function $C(A_{\rm tot})^{\tau}$, where C and τ are the fitting parameters.

In figure 4, we show the elliptic flow V_2 for the midrapidity region ($-0.3 \leq Y \leq 0.3$) for $2 \leq A \leq 4$ as a function of the incident energy. The rapidity cut is in accordance with the experimental findings. The theoretical results are compared with the experimental data extracted by the 4π Array group [31]. For comparing calculations with experimental findings, we have performed the detailed analysis by taking into account static equations of state. The comparison has been done at the same impact parameter as calculated in [17,31,32] after correction. The general behaviour of the elliptic flow calculated with different EOSs resembles each other. The elliptic flow evolves from a preferential in-plane (rotational like) emission ($V_2 > 0$), to the out-of-plane (squeeze-out) emission ($V_2 < 0$), with an increase in the incident energies. The elliptic flow decreases with the incident energy. The decrease in elliptic flow is sharp at smaller incident energies (upto 65 MeV/nucleon). This starts saturating at higher incident energies. In other words, the elliptic shape of the nuclear flow dominates the physics at low incident energies. One can see from the figure that the transition energies at which the elliptic flow parameter V_2 changes sign from positive to negative are different for different equations of state. The transition from the in-plane emission to out-of-plane emission occurs because the mean field that contributes to the formation of the compound nucleus becomes less important. At the same time, the collective expansion process (based on the nucleon–nucleon scattering) starts dominating. The competition between the mean-field and the nucleon–nucleon collisions strongly depends on the effective interactions, which leads to the divergence of the transition energies calculated with hard and soft equations of state. Clearly, the hard EOS provides stronger pressure that leads to a stronger out-of-plane emission and thus to smaller transition energy. The difference of elliptic flow between hard and soft EOSs decreases as we move towards higher incident energies. The elliptic flow calculated with hard equation of state agrees with the 4π Array experimental data. From our analysis, we find that hard equation of state explains the data closely.

4. Summary

We presented the systematic theoretical results on elliptic flow by analysing nearly symmetric reactions, e.g., ${}_{10}\mathrm{Ne}^{20} + {}_{13}\mathrm{Al}^{27}$, ${}_{18}\mathrm{Ar}^{40} + {}_{21}\mathrm{Sc}^{45}$, ${}_{30}\mathrm{Zn}^{64} + {}_{28}\mathrm{Ni}^{58}$, ${}_{36}\mathrm{Kr}^{86} + {}_{41}\mathrm{Nb}^{93}$ at incident energies between 45 and 105 MeV/nucleon and over full geometrical overlap within the framework of QMD model. The general features of the elliptic flow were investigated with the help of theoretical simulations, particularly, the transverse momentum, impact parameter, system size dependence and incident energy dependence. Special emphasis was put on the energy dependence of the elliptic flow. We also compared our theoretical calculations with 4π Array data. This comparison, performed for the reaction of ${}_{18}\mathrm{Ar}^{40} + {}_{21}\mathrm{Sc}^{45}$ showed that the hard equation of state explains the data clearly. In general, a good agreement was obtained between the data and calculations. We also predicted that elliptic flow for different fragments follows power-law dependence as given by the function $C(A_{\rm tot})^{\tau}$.

Acknowledgement

This work was supported by the grant from the Department of Science and Technology (DST), Government of India vide Grant No. SR/WOS-A/PS-10/2008.

References

[1] R K Puri *et al*, *Nucl. Phys.* **A575**, 733 (1994)
ibid., Phys. Rev. **C54**, R28 (1996)
Ch Hartnack *et al*, *Eur. Phys. J.* **A1**, 151 (1998)
J K Dhawan *et al*, *Phys. Rev.* **C74**, 054610 (2006)
[2] G F Bertsch and S Das Gupta, *Phys. Rep.* **160**, 189 (1988)
[3] J Aichelin, *Phys. Rep.* **202**, 233 (1991)
[4] D T Khoa *et al*, *Nucl. Phys.* **A548**, 102 (1992)
G Batko *et al*, *J. Phys. G: Nucl. Part. Phys.* **20**, 461 (1994)
E Lehmann *et al*, *Phys. Rev.* **C51**, 2113 (1995)
S Kumar and R K Puri, *Phys. Rev.* **C58**, 1618 (1998)
E Lehmann *et al*, *Z. Phys.* **A355**, 55 (1996)
[5] A D Sood *et al*, *Phys. Rev.* **C70**, 034611 (2004)
ibid., **C79**, 064618 (2009)
ibid., **C73**, 067602 (2006)
S Gautam *et al*, *J. Phys.* **G37**, 085102 (2010)
S Kumar *et al*, *Phys. Rev.* **C58**, 3494 (1998)
A D Sood and R K Puri, *Phys. Lett.* **B594**, 260 (2004)
S W Huang *et al*, *Prog. Part. Nucl. Phys.* **30**, 105 (1993)
[6] L G Moretto and G J Wozniak, *Nucl. Part. Sci.* **43**, 379 (1993)
[7] J Y Ollitrault, *Phys. Rev.* **D46**, 229 (1992)
[8] H Sorge, *Phys. Rev. Lett.* **78**, 2309 (1997)
[9] Ch Hartnack, H Oeschler and J Aichelin, *J. Phys.* **G35**, 044021 (2008)
[10] S Voloshin and Y Zhang, *Z. Phys.* **C70**, 665 (1996)
[11] H Stöcker and W Greiner, *Phys. Rev. Lett.* **44**, 725 (1980)
[12] H Stöcker *et al*, *Phys. Rev.* **C25**, 1873 (1982)
[13] M B Tsang *et al*, *Phys. Rev.* **C53**, 1959 (1996)
[14] A B Larionov, W Cassing, C Greiner and U Mosel, *Phys. Rev.* **C62**, 064611 (2000)
[15] C Alt *et al*, *Phys. Rev.* **C68**, 034903 (2003)
[16] Y M Zheng, C M Ko, B A Li and B Zhang, *Phys. Rev. Lett.* **83**, 2534 (1999)
[17] G D Westfall *et al*, *Nucl. Phys.* **A681**, 343 (2001)
ibid., Phys. Rev. Lett. **71**, 1986 (1993)
[18] M Gyulassy, K A Frankel and H Stöcker, *Phys. Lett.* **B110**, 185 (1982)
[19] J Gosset *et al*, *Phys. Rev.* **C16**, 629 (1977)
J Pluta *et al*, *Nucl. Phys.* **A562**, 365 (1993)
[20] H H Gutbrod *et al*, *Phys. Rev.* **C42**, 640 (1990)
ibid., Phys. Lett. **B216**, 267 (1989)
[21] R Popescu *et al*, *Phys. Lett.* **B331**, 285 (1994)
[22] J Lukasik *et al*, *Phys. Lett.* **B608**, 223 (2005)
[23] A Andronic *et al*, *Nucl. Phys.* **A679**, 765 (2001)
S Kumar *et al*, *Phys. Rev.* **C81**, 014611 (2010)
ibid., **C81**, 014601 (2010)
ibid., **C78**, 064602 (2008)

[24] Y Zhang and Li Zhuxia, *Phys. Rev.* **C74**, 014602 (2006)
[25] H Y Zhang *et al*, *Eur. Phys. J.* **A15**, 399 (2002)
H Peterson *et al*, *Phys. Rev.* **C74**, 064908 (2006)
D Persram and C Gale, *Phys. Rev.* **C65**, 064611 (2002)
[26] A Bohnet, N Ohtsuka, J Aichelin, R Linden and A Fasseler, *Nucl. Phys.* **A494**, 349 (1989)
[27] Ch Hartnack, J Aichelin, H Stöcker and W Greiner, *Phys. Lett.* **B336**, 131 (1994)
[28] Y K Vermani and R K Puri, *Eur. Phys. Lett.* **85**, 62001 (2009)
ibid., Phys Rev. **C79**, 064613 (2009)
ibid., Nucl. Phys. **A847**, 243 (2010)
R K Puri *et al*, *Phys Rev.* **C57**, 2744 (1998)
R K Puri *et al*, *J. Comput. Phys.* **162**, 245 (2000)
J K Dhawan and R K Puri, *Phys. Rev.* **C75**, 057901 (2007)
[29] M Colona *et al*, *Catania Workshop on Nucleon and Neutrino Astrophysics*, 15–16 Feb., 2007
M D Toro *et al*, *Eur. Phys. J.* **A30**, 153 (2006)
[30] T Z Yan *et al*, *Chin. Phys.* **16**, 2676 (2007)
[31] D J Magestro, *Transitions of collective flow observables at immediate energies*, Ph.D. Thesis (Michigan State University, 2000)
[32] R Pak *et al*, *Phys. Rev.* **C54**, 2457 (1996)
ibid., **53**, R1469 (1996)